

A Novel Control Strategy For Active Power Filter In Grid-Connected PV System Under Unbalanced And Distorted Grid Voltages

Mouna Tali, Tamou Nasser, Ahmed Essadki

Abstract: Remarkable growth of grid-connected renewable sources like PV systems imposes the use of power electronics converters (mainly PV inverters) in order to ensure efficient and reliable power conversion and grid synchronization. Therefore, under non ideal voltage conditions, the controller design of the PV inverter incorporating Shunt Active Power Filter functionality, becomes a significant challenge for power quality enhancement. On that account, this paper proposes a new concept of Direct Power Control (DPC) with an optimal switching table using extended PQ theory, which is suitable to compensate reactive power and eliminate harmonics drawn by nonlinear loads. Moreover, comparative study with the conventional DPC control strategy is presented to verify the superiority and the performance of the proposed DPC. Simulation results with Matlab/Simulink show that the proposed DPC is able to improve power quality under undesirable voltage supply conditions.

Index Terms: Direct Power Control; Active Power Filter; Grid Connected PV System; MPPT; THD.

1. INTRODUCTION

Recently, power quality presents a technical challenge and attracts more attention, due to the extensive usage of the nonlinear loads such as: electric arc furnace, static VAR compensators, and motor drives. These nonlinear loads generate harmonics in the line currents, consume reactive power, and decrease the reliability of power systems. [1,2] To need to produce pollution-free energy has triggers great efforts toward renewable energy systems like wind and solar energy. Grid-connected PV generator becomes more practical and popular due to its reliable performance. In the association of the PV generator to the grid, power electronic converters are required to convert PV DC power into AC power for utility or supplying local loads. The inverter function is to inject into the grid a sinusoidal current with phase and frequency equal to the corresponding grid voltage, on the other hands, with the presence of the nonlinear loads, the inverter can provide the harmonic elimination by injecting compensating current through flexible and efficient control. Therefore, the integration of PV generator into power system requires consideration of fast voltage regulation, synchronization, stability and power quality problems. Active Power Filters (APFs) (such as shunt APFs, series APFs, hybrid APFs, unified power quality conditioner UPQC) are adopted and seem to become the most effective solution to mitigate harmonics and to enhance the power quality [3, 4, 5]. In grid connected PV system, SAPF is asked to act as a multifunctional PV inverter which has abilities to inject active power to the loads or/and to the grid and to compensate power factor simultaneously with low cost and lower total harmonic distortion THD, through reliable current control strategy. Even in the absence of solar energy, the SAPF can still operate to improve the power quality. The IEEE 519 standard recommends that the total harmonic distortion THD of the line current must be less than 5%. Various control strategies have been proposed to control shunt active power filter SAPF in grid connected PV system: Instantaneous pq theory is applied to design the PV-APF controller in [6], the PV power has been injected correctly and the utility currents have been compensated successfully with the current THD value equal to 3.67%. In [7] harmonic current damping and reactive power compensation are achieved using synchronous reference frame theory and the current THD is reduced to 2.87%. In [8] a comparison with sliding mode

controller and hysteresis controller in APF-PV combination is studied, good steady state and fast dynamic response are achieved and the current THD is decreased to 3.24% in sliding mode. Authors are employed the direct control power DPC in APF-PV controller without voltage sensors [9], better compensation is observed in the line current and the THD value is equal to 1.5%. Artificial neural networks technics, fuzzy logic control, genetic are discussed in [10..12]. So far, the majority of control strategies for APF-PV combination are made in normal network conditions and have limited efficiency when the grid voltages are unbalanced or distorted which can degrade the electric system reliability and causes a poorer power quality. Therefore, the control methods of active power filter under unbalanced grid voltages have become an interesting concern [13, 14]. In this paper DPC is employed to control Shunt active power filter in grid connected PV system thanks to its simplicity and rapid dynamic response [15..18]. To be operating under unbalanced grid voltages, the proposed DPC controller is based on a new definition of reactive power called extended power theory developed by Komatsu [19].

2 PV SYSTEM CONFIGURATION

D Figure 1 describes the envisaged system of the grid connected PV system. PV generator is connected to the utility via DC / AC Converter. To adapt the DC voltage to a desired level for PV inverter, DC / DC converter is required. To verify the multifunctionality of the PV inverter, the nonlinear load is connected to the grid, in this case as for an APF; it must be able ensure power quality by injecting the compensating currents at the PCC.

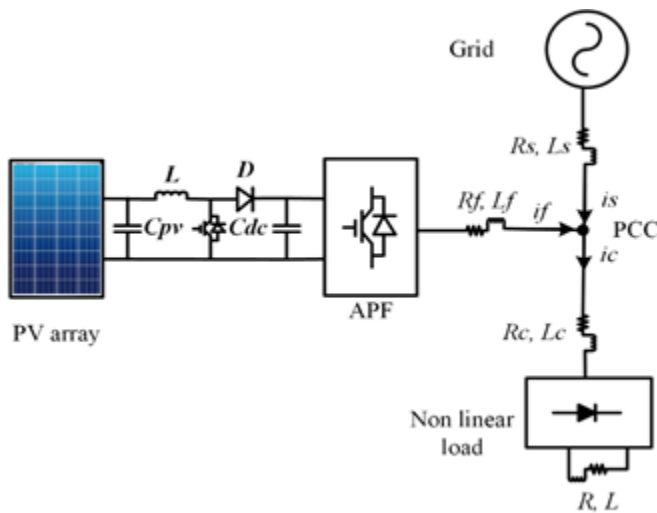


Fig. 1. The proposed grid connected PV system

3 CONTROL STRATEGY OF SHUNT ACTIVE POWER FILTER (SAPF)

SAPF is a VSI inverter connected in parallel with the non-linear load and the network at the PCC, it is able to provide the following features: harmonics mitigation, reactive power compensation and solar power injection. An effective control strategy remains the key to achieve these goals. A new control strategy based on DPC with a new switching table using the PQ extension theory is shown in Figure 2.

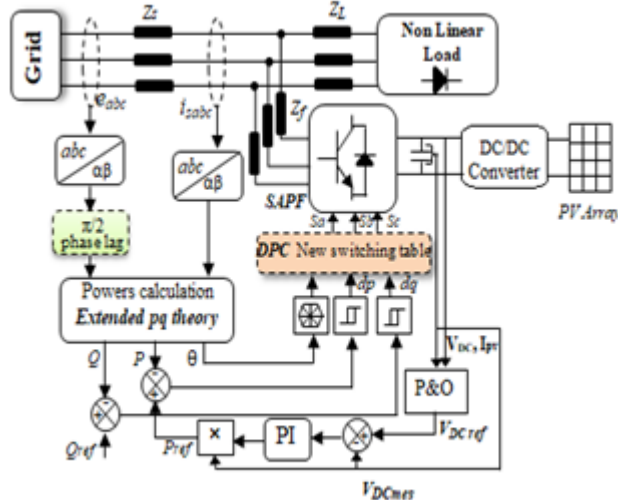


Fig.2. Control structure based DPC of the proposed system. DPC Control

3.1 DPC Control

DPC control based on the principle of direct torque control DTC strategy applied in electrical machines control has become an interesting control strategy in many application [21,22]. In this method, the converter switching states are selected from a look up table based on errors of both of active and reactive powers and the vector voltage position without any inner current control and PWM modulator. The basic idea of DPC is to choose the best state of the power switches among the twelve possible states in order to follow the reference powers. The active power reference is obtained from an outside DC voltage PI controller, the reactive power must

be kept to zero value to achieve unity power factor. The errors of the active and reactive powers are obtained by hysteresis blocks [15..19]. The conventional DPC strategy based on pq theory gives satisfactory performances as long as the supply voltage is ideal, but when this condition is not verified and distortion or unbalance affect the grid voltages, the performance will degrade severely, for this reason, the motivation in this paper is to extended the performance of DPC to be operate under unbalanced grid voltages. So to achieve this aim the extended pq theory is used in the proposed DPC control strategy. The instantaneous active and reactive powers can becalculated using equations (2) based on the instantaneous power pq theory [3]:

$$S = p + jq \tag{1}$$

$$\begin{bmatrix} p \\ q \end{bmatrix} = \begin{bmatrix} e_{\alpha} i_{\alpha} + e_{\beta} i_{\beta} \\ e_{\beta} i_{\alpha} - e_{\alpha} i_{\beta} \end{bmatrix} \tag{2}$$

The control system is designed in $\alpha\beta$ reference frame; hence, Clarke transformation is needed to transform the variables between abc and $\alpha\beta$ coordinates

$$\begin{bmatrix} x_{\alpha} \\ x_{\beta} \end{bmatrix} = \sqrt{\frac{2}{3}} \begin{bmatrix} 1 & -\frac{1}{2} & -\frac{1}{2} \\ 0 & \frac{\sqrt{3}}{2} & -\frac{\sqrt{3}}{2} \end{bmatrix} \begin{bmatrix} x_a \\ x_b \\ x_c \end{bmatrix} \tag{3}$$

where $x \in [e, i]$

The novel reactive power defined in extended pq theory is defined as [19]:

$$q^{nov} = e'_{\alpha} i_{\alpha} + e'_{\beta} i_{\beta} \tag{4}$$

Where e' denotes the quadrature voltage lagging e by 90 degrees.

Fig. 3 shows the equivalent circuit of the SAPF connected to the grid and the nonlinear load per phase, the relationship between the grid voltage and grid current by neglecting resistors R_s and R_f can be expressed as:

$$e_{\alpha\beta} = L_s \frac{di_{\alpha\beta}}{dt} + v_{f\alpha\beta} - L_f \frac{di_{\alpha\beta}}{dt} \tag{5}$$

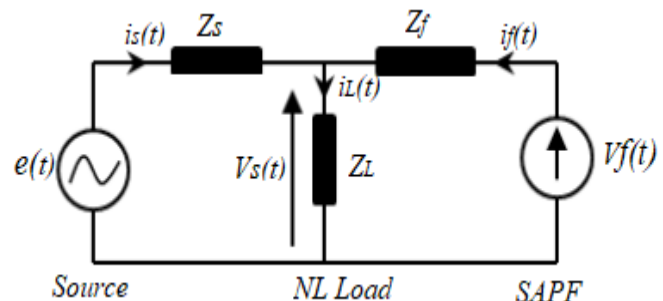


Figure. 3. Equivalent circuit topology. The selection of the voltage vectors of the active power filter

from the switching table is based on the evolution of the variation of active power and reactive power. By deriving equations 2 and 4, the variation of active and reactive powers can be expressed as:

$$\frac{dp}{dt} = e_\alpha \frac{di_\alpha}{dt} + i_\alpha \frac{de_\alpha}{dt} + e_\beta \frac{di_\beta}{dt} + i_\beta \frac{de_\beta}{dt} \tag{6}$$

$$\frac{dq^{nov}}{dt} = e'_\alpha \frac{di_\alpha}{dt} + i_\alpha \frac{de'_\alpha}{dt} + e'_\beta \frac{di_\beta}{dt} + i_\beta \frac{de'_\beta}{dt} \tag{7}$$

$$\frac{de_\alpha}{dt} = -\omega e_\beta; \frac{de_\beta}{dt} = +\omega e_\alpha; \frac{de'_\alpha}{dt} = \omega e_\beta \tag{8}$$

The derivatives of grid currents in the stationary frames $\alpha\beta$ can be obtained using following equation:

$$\frac{di^{\alpha\beta}}{dt} = \frac{1}{L_s + L_f} (e^{\alpha\beta} - v_f^{\alpha\beta}) \tag{9}$$

According equations (6) to (9) and (11,12) the variation of active and the novel reactive power for different converter voltage vectors can be calculated and illustrated in figure 4. The VDC is the dc link voltage and V_f is the converter voltage vector $V_f = \frac{2}{3}V_{dc} e (j \frac{\pi}{3(n-1)}) (n=1,2...6)$, $e = \|e\|$ and θ is the angular position of the grid voltage vector in $\alpha\beta$ coordinates defined as:

$$\theta = \text{artan}^{-1} \left(\frac{e_\beta}{e_\alpha} \right) \tag{10}$$

$$\frac{dp}{dt} = K \left(K' - \cos \left(\theta - (n-1) \frac{\pi}{3} \right) \right) - \omega q \tag{11}$$

$$\frac{dq^{nov}}{dt} = -K \left(\sin \left(\theta - (n-1) \frac{\pi}{3} \right) \right) + \omega p \tag{12}$$

where: $K = \frac{\|e\|}{L_s + L_f} \sqrt{\frac{2}{3}} V_{dc}$, $K' = \frac{\|e\|^2}{L_s + L_f}$

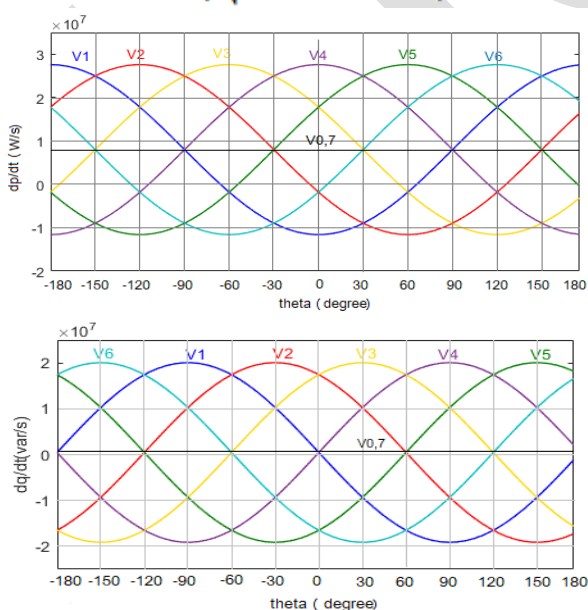


Figure. 4. Instantaneous power variations for different

voltage vectors.

The optimal inverter voltage vector can be selected to adjust the active power and the reactive power from the new switching table which elaborated depending the output of the hysteresis comparators dp , dq and the voltage vector position as defined as:

$$(n-1) \frac{\pi}{6} \leq \theta_n \leq n \frac{\pi}{6} \tag{13}$$

$$dp = \begin{cases} 1 & \text{if } P_{ref} - P \geq hp \\ 0 & \text{if } P_{ref} - P \leq hp \end{cases}$$

$$dq = \begin{cases} 1 & \text{if } Q_{ref} - Q \geq hp \\ 0 & \text{if } Q_{ref} - Q \leq hp \end{cases}$$

For this purpose, the working plane (α, β) is divided in 12 sectors (see Fig. 5):

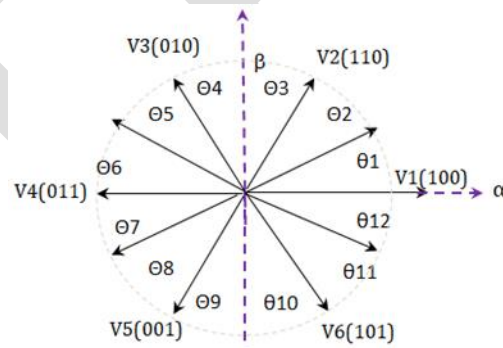


Figure.5. Sectors classification for DPC in stationary $\alpha\beta$ frame.

The reference power is delivered from the DC bus voltage controller, however, the reactive power is set to zero to get unity power factor. To obtain the switching table for the DPC control, four combinations of active and reactive power variation are available and by examining figure 4, we can see that are several voltage vector possibilities for a particular combination of power variation for each angular position. However, only one suitable voltage vector should be chosen for a particular combination of power variation which produce much lower active power and reactive power variation (dp/dt_{min}) and (dq/dt_{min}) to minimize the errors between reference and the measured active power and reactive power. For example, in the first sector ($0..30^\circ$) in case ($dp>0$ and $dq>0$) both of vectors $V3$ and $V4$ can be chosen and for ($dp<0$ and $dq<0$) both of $V1$ and $V6$ can be chosen. The influence of converter voltage vector on error active power and reactive power in other sectors can be analyzed similarly. The classical switching table developed by Nogushi has always given the satisfactory performance when the grid voltage is balanced, however, under several grid voltage conditions, power fluctuations and harmonics currents can be presented therefore, the new switching table using the extended reactive power elaborated in table2 deal for good performance

Table1. Conventional DPC

dp	dq	θ_1	θ_2	θ_3	θ_4	θ_5	θ_6	θ_7	θ_8	θ_9	θ_{10}	θ_{11}	θ_{12}	
0	0	1	V_1	V_1	V_2	V_2	V_3	V_3	V_4	V_4	V_5	V_5	V_6	V_6
0	1	V_6	V_6	V_1	V_1	V_2	V_2	V_3	V_3	V_4	V_4	V_5	V_5	V_6
1	1	V_7	V_7	V_0	V_0	V_7	V_7	V_0	V_0	V_5	V_5	V_7	V_0	V_0
1	1	V_0	V_0	V_6	V_6	V_7	V_7	V_3	V_3	V_0	V_4	V_4	V_7	V_5

Table2. Proposed DPC

dp	dq	θ_1	θ_2	θ_3	θ_4	θ_5	θ_6	θ_7	θ_8	θ_9	θ_{10}	θ_{11}	θ_{12}
0	0	V_1	V_1	V_2	V_2	V_3	V_3	V_4	V_4	V_5	V_5	V_6	V_6
0	1	V_2	V_2	V_3	V_3	V_4	V_4	V_5	V_5	V_6	V_6	V_1	V_1
1	0	V_5	V_5	V_6	V_6	V_1	V_1	V_2	V_2	V_3	V_3	V_4	V_4
1	1	V_3	V_3	V_4	V_4	V_5	V_5	V_6	V_6	V_1	V_1	V_2	V_2

4. RESULTS AND DISCUSSION

The performance of the present SAPF controller using the proposed DPC is verified with Matlab /Simulink, a comparison with the conventional DPC is presented under unbalanced and distorted grid voltage conditions. The challenge of the whole system is to achieve sinusoidal and balanced grid current while keeping perfect transfer of solar power from PV array to the grid and to the load with unity power factor following $Q_{ref} = 0VAR$. An irradiation profile showed in figure 6(a) is suggested to reveal the behavior of SAPF in grid connected PV- system. For modeling the PV system, the Sx-60 a typical 60w PV module was chosen, the key specification are shown in table 3.

Table3. SX-60 PV ARRAY Parameters

Description	Value
Ideality factor	$a=1.2$
Maximum Power	$P_{max}=60W$
Voltage at P_{max}	$V_{max}=16.8V$
Current at P_{max}	$I_{max}=3.59A$
Short-circuit current	$I_{sc}=3.87A$
Open circuit voltage	$V_{oc}=21.06V$
Parallel connected modules	$N_p=1$
Series connected cells	$N_s=36$

The parameters simulation are shown in table 4.

Table4. System Parameters Simulation

Parameters	Values
V_s, f_s	100v, 50Hz
L_s, R_s	10 μ H, 0.1 Ω
L_L, R_L	10mH, 30 Ω
L_f, R_f	8mH, 0.01 Ω
C_{dc}, V_{dc}	2200 μ F, 300v
K_p, K_i	2, 0.008

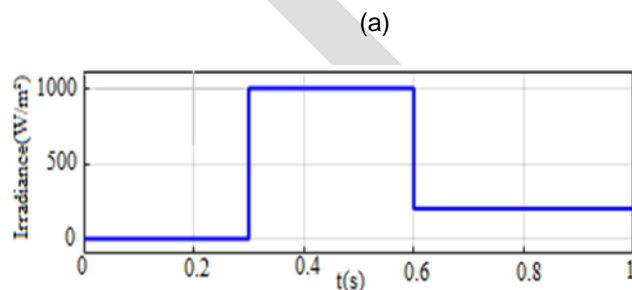


Figure 6 (a). Solar irradiation. PV current.

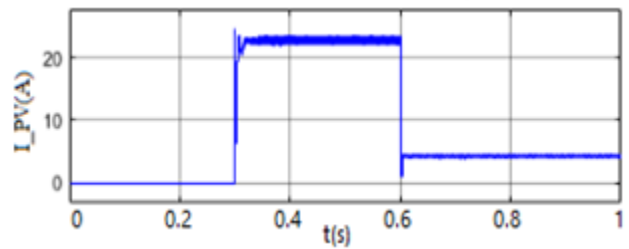


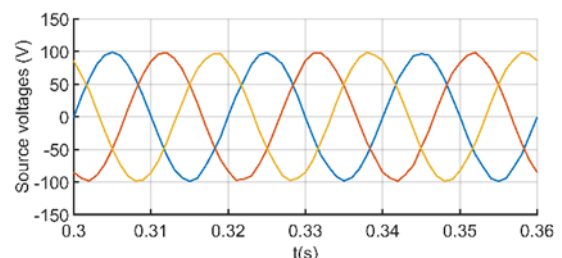
Figure 6 (b) depicts current generated by the PV array.

To verify the robustness of the proposed DPC in the multifunctional system, three different cases of grid voltage conditions have been studied.

Case A: Sinusoidal and balanced grid voltages

Figures 7 to 15 shows the simulation results under balanced and sinusoidal grid voltages for proposed DPC PDPC, in the first case, without SAPF compensation, the source currents are distorted severely and the THD is equal to 25.8%. After SAPF compensation, it is seen in figure 8(a) that the grid current becomes balanced and in phase with the grid voltage, the compensating currents injected by the SAPF at the PCC are depicted in figure 8(b). Figures 9 shows the behavior of the active and reactive powers of the whole system, active power of the grid (P_s), the non-linear active power (P_L) and the power injecting by the PV system (P_f). The negative value of the active power P_s (at $W=1000w/m^2$) means that the PV power is higher than the power demanded by the load. So the PV power feeds the load and the excess is injected correctly to the grid, which is exhibited by the opposite sign of the source current and source voltage in figure 8(b). After $t=0.6s$, the solar irradiation decrease to $200w/m^2$, in this case the load is supplied from the grid and the PV system simultaneously.

(a)



(b)

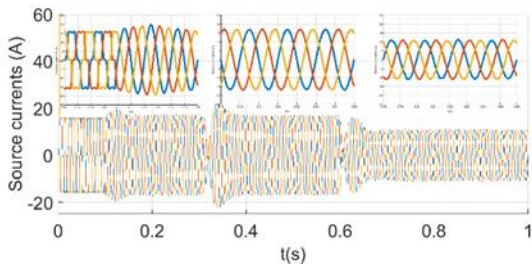


Figure 7(a) Grid voltage, (b) Grid voltage with grid current with PDPC.

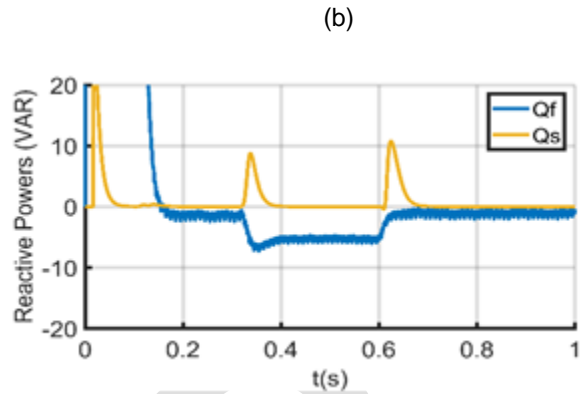
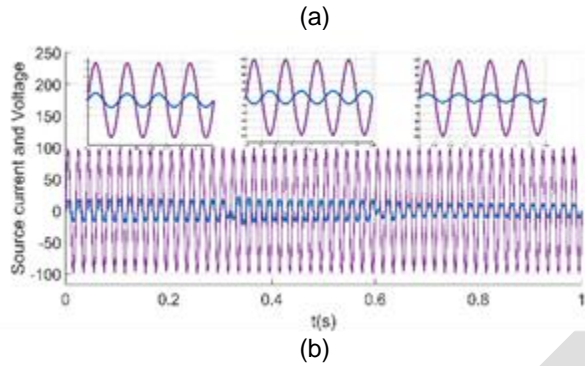
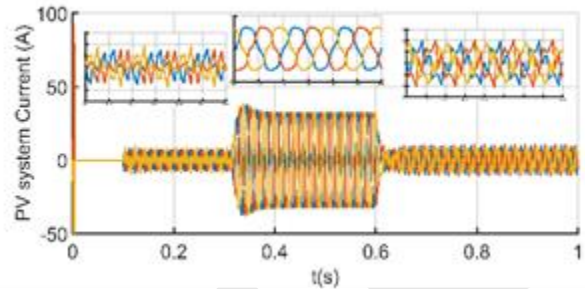


Figure 9. (a) Active powers in PDPC, (b) reactive powers in PDPC



(b)



(a)

Figure 8 (a) Grid currents (b) Compensating currents with PDPC

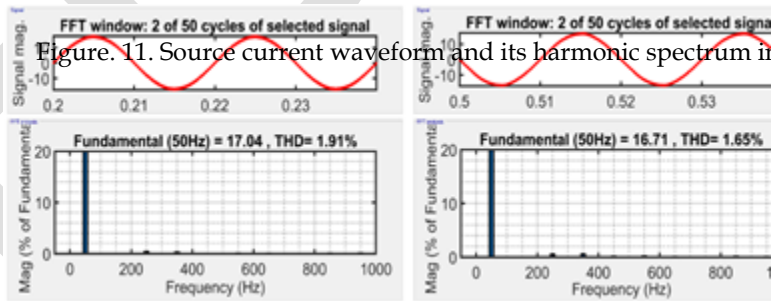


Figure 11. Source current waveform and its harmonic spectrum in

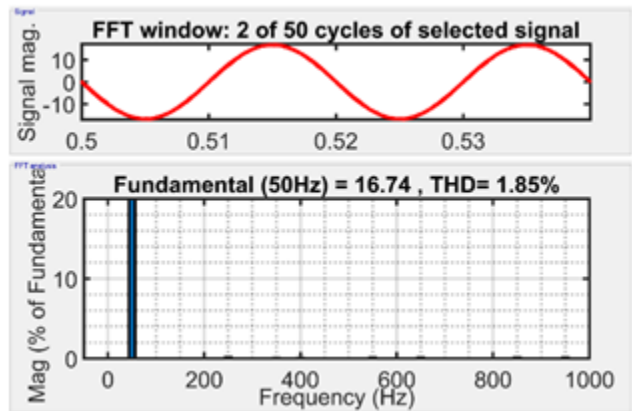


Figure 12. Source current and harmonic spectrum with CDPC.

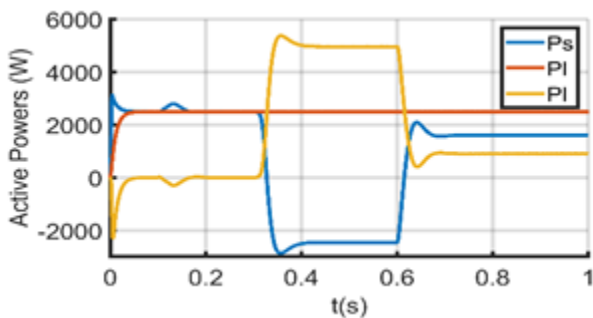


Figure 10 shows the behavior of the DC link voltage; we can see from this response that the voltage follows perfectly its reference at the steady state. Under rapidly change of irradiation at $t=0.3s$ and at $t=0.6s$, two oscillations can be

observed due to exchange of powers between the grid and PV system.

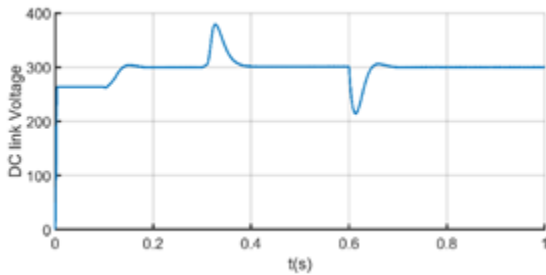
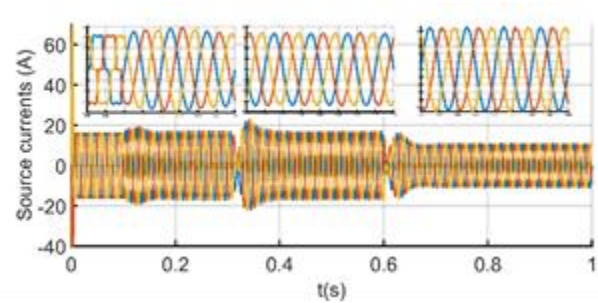


Figure.10. DC capacitor voltage in PDPC.

Figure 11 and 12 depict source current waveforms and their harmonic spectrums under variable solar irradiance for PDPC and CDPC respectively, it is clearly seen that under balanced grid voltage conditions, both of methods are almost the same results and the current THD is reduced to (THDPDPC = 1.65% ; THDCDPC = 1.85%).

□ Case B: Unbalanced sinusoidal grid voltages

To verify the efficiency of the proposed PDPC algorithm, an unbalanced system is applied, the phase (a) has different magnitude by 15% compared to the other phases (b) and (c) as depicted in Figure 13(a). CDPC Method behavior in this conditions is shown in Figure 18, it exhibits that the source currents are widely distorted with a THD value equal to 6.69%. This method confirms its limitation under unbalanced grid voltages. On the other hands, the proposed PDPC algorithm using the extended pq theory gives good results, the source currents are balanced and have the same magnitude during a solar irradiance changing, this is noticed in the figure 13(b). The THD is improved to a lower value as presented in Fig. 13. It can be seen in figure 14(a), that not only the power delivered by the PV system can supply local loads but also it can inject the surplus of the power to the grid at the fort irradiation ($G=1000w/m^2$) and in figure 14(b), it is observed that the new reactive power stills constant and tracks its reference 0VAR to achieve unity power factor under unbalanced voltage conditions.



(c)

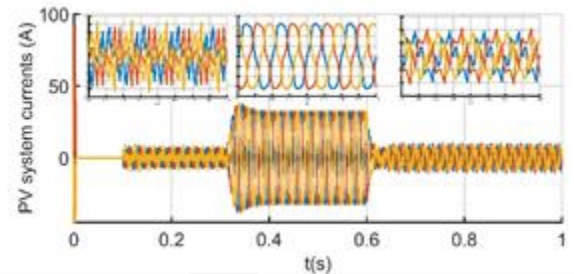
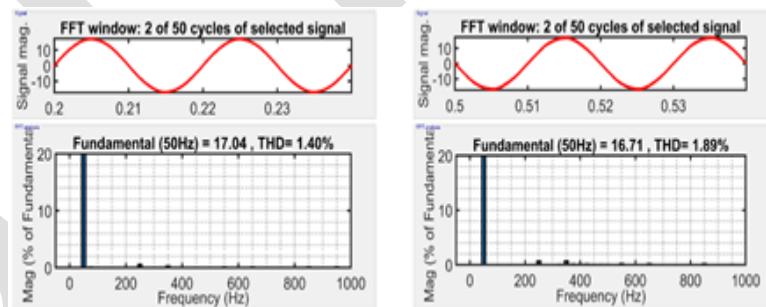
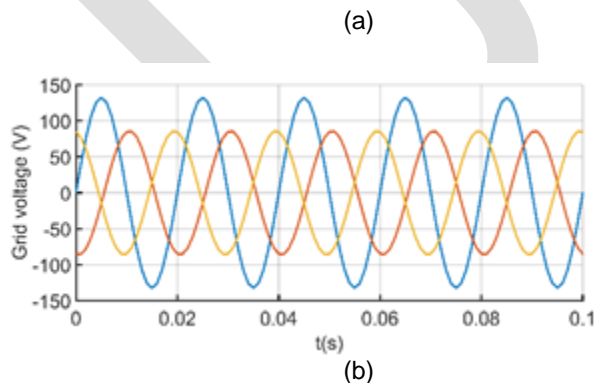


Figure 13 (a) grid voltages, (b) grid currents and (c) compensating currents with PDPC under unbalanced source voltages.

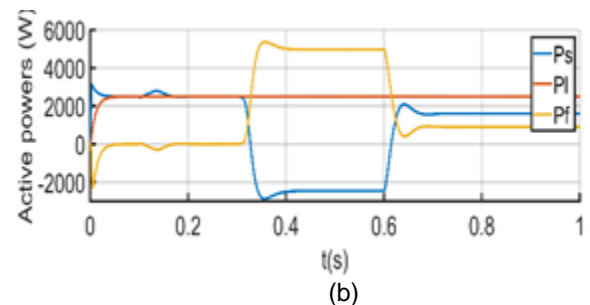


(a)

Figure. 16. Source current waveform and harmonic spectrum in phase (a) before and after SAPF with PDPC under unbalanced grid voltages.



(b)



(b)

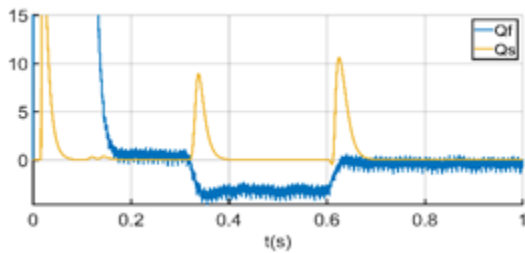
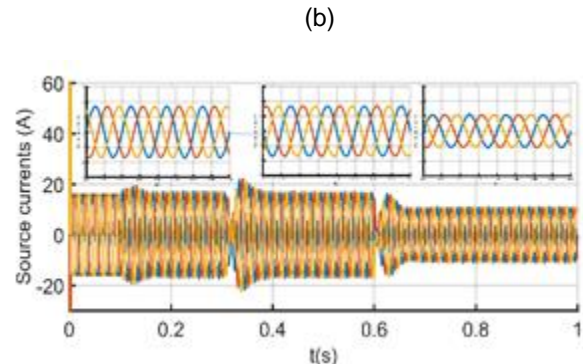


Figure 14. (a) Active powers, (b) reactive powers with PDPC



(b)

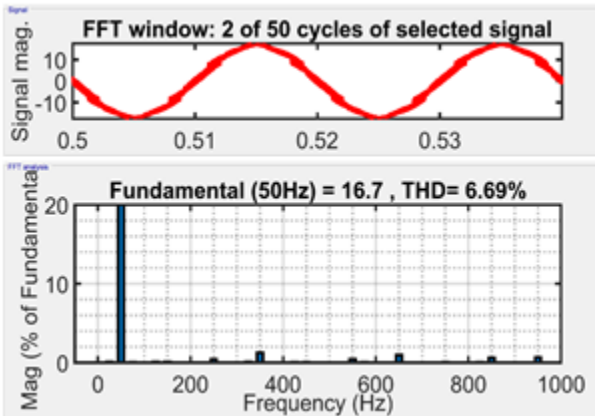
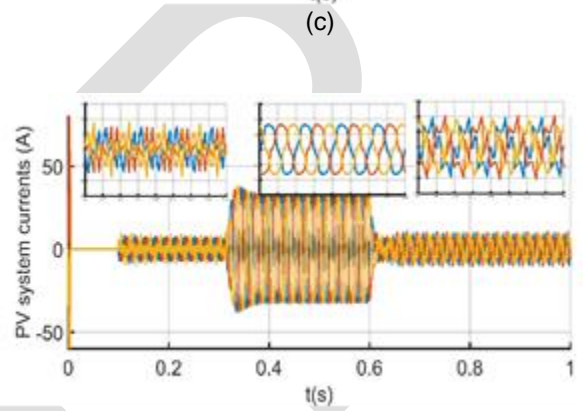


Figure 15. Source current and harmonic spectrum with CDPC

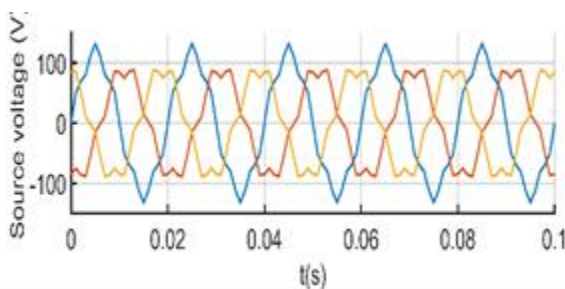


(c)

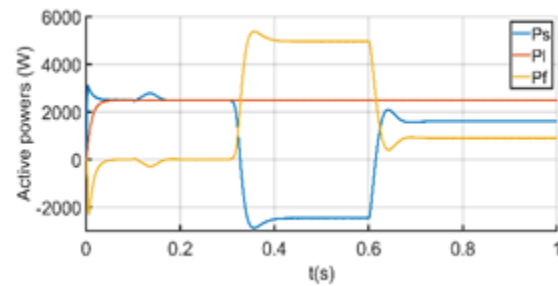
The effectiveness of the proposed PDPC under distorted and unbalanced grid voltages is confirmed by good quality of the current waveform in terms of Total Harmonic Distortion THDPDPC = 1.89 % in all operation modes as shown in Figure 18. Figure 19 exhibits the superiority of the PDPC against CDPC, which is clearly observed in the THD value (THDCDPC=6.72%).

□ Case C: Distorted and unbalanced grid voltages
 In this case, grid voltages are purely distorted, the fifth harmonic component with 10% of the magnitude of fundamental is present in grid voltages. The performance of the proposed DPC control is widely observed in Figure 17(b). We can see that the source currents become purely sinusoidal and the harmonics are completely eliminated by injecting compensating current at the PCC as shown in figure 17(c). In Figure 17(d, e) active and reactive powers of the utility and the nonlinear load are depicted respectively before and after filtering during solar irradiance changing. They follow their references value perfectly under the distorted conditions with a unity power factor.

(a)



(d)



(e)

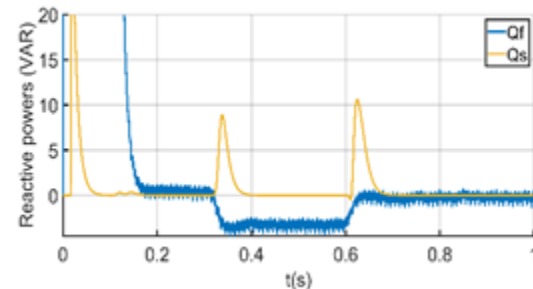


Figure 17. (a) grid voltages, (b) grid currents, (c)

compensating currents, (d) active powers, (e) reactive powers.

proposed PDPIC technique proves the excellent performances under any faults in grid voltages which confirmed by the previous results simulations.

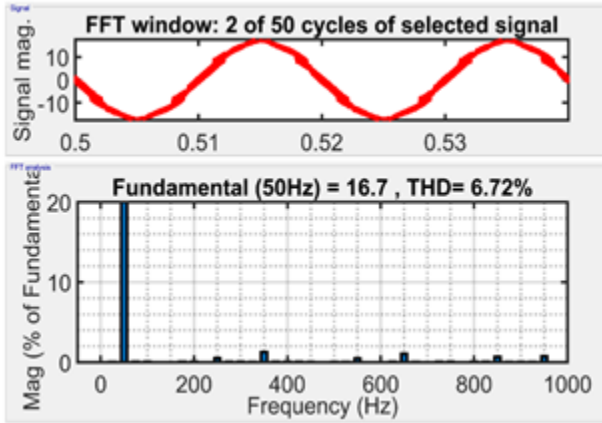


Fig.18. Source current and harmonic spectrum with CDPC

Figure. 19. Source current waveform and harmonic spectrum in phase (a) before and after SAPF with PDPIC under solar irradiance change

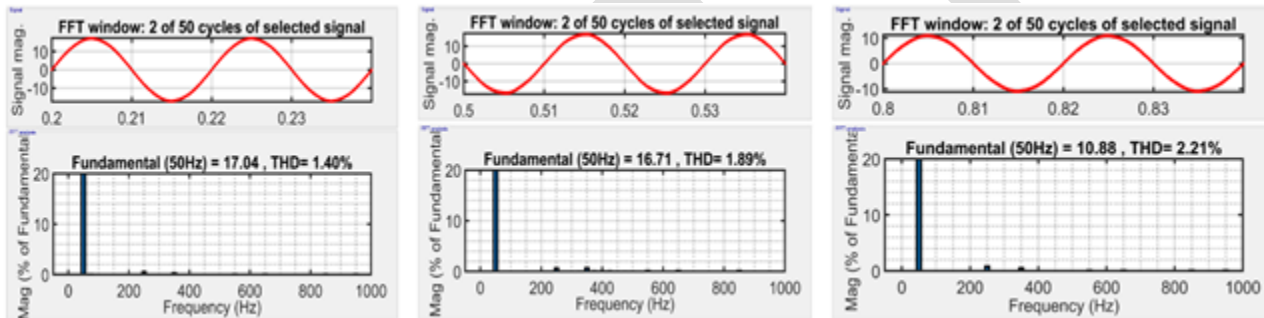


Table 4 presents the obtained results of THD currents under various conditions of grid voltages; balanced, unbalanced, unbalanced and distorted voltages cases. As shown in obtained simulation results, the best compensation in term of power quality enhancement is confirmed by the proposed PDPIC method

Table.4. Comparison of currents THD within PV system Control:

Grid voltage Conditions	CDPC	PDPIC
Balanced	1.85%	1.65%
unbalanced	6.69 %	1.89%
unbalanced/distorted	6.72%	1.89%

5. CONCLUSION

In this paper, a novel switching table based DPC controller suitable to control shunt active power filter in grid connected PV system under unbalanced and distorted grid voltages is proposed. Using a new reactive power based on extended pq theory, mitigation of harmonics, compensation of reactive power and correct injection of solar power are achieved at variable solar irradiances using the optimal MPPT algorithm. When the grid voltage is balanced and sinusoidal without any faults, the DPC using conventional pq theory gives always the satisfactory performances, but when one of one of the conditions already mentioned is missing, the controller based conventional DPC is not efficient and the several degradations can dab power quality. Compared to conventional CDPC, the

REFERENCES

- [1] A. Arash, A Sarwat, "Overview of technical specifications for grid-connected photovoltaic systems," Energy Conversion and Management, Vol. 15, no. 2, pp. 312-327, 2017.
- [2] S. Saridakis, E. Koutroulis, "Optimal Design of Modern Transformerless PV Inverter Topologies", IEEE Transactions on Energy Conversion. 22 May 2013.
- [3] H.Akagi. "New Trends in Active Filters for Power Conditioning", IEEE. 0093-9994/9605.00 1996.
- [4] H. Akagi, Y. Kanazawa, and A. Nabae, "instantaneous reactive power compensators comprising switching devices without energy storage 5. components,"IEEE. Ind. Appl, vol. 20, no. 3, pp. 625-630, 1984.
- [5] A.Teke, L.Saribulut, M.E.Meral, M.Tumay, "Acive Power Filter: Review of converter Topologies and Control Strategie", GUJS, vol 24, pp. 283-289, 2011.
- [6] N. D.Tuyen, G. Fujita, "PV-Active Power Filter Combination Supplies Power to Nonlinear Load and Compensates Utility Current", IEEE Power and Energy Technology Systems Journal, Vol. 2, Issue: 1, pp. 32 - 42 March 2015.
- [7] R. Belaidi, A. Haddouche, M. M. Larafi, "Shunt active power filter connected to a photovoltaic array for compensating harmonics and reactive power simultaneously", 4th International Conference on Power Engineering, Energy and Electrical Drives, pp. 1482-

- 1486, Istanbul, Turkey.
- [8] A. Bag, B. Subudhi, P. K. Ray, "Comparative Analysis of Sliding Mode Controller and Hysteresis Controller for Active Power Filtering in a Grid connected PV System", *International Journal of Emerging Electric Power Systems*, vol.19, pp. 1-13, 2018.
- [9] Z. Chelli, A. Lakehal, T. Khoualdia, Y. Djeghader, " Study on Shunt Active Power Filter Control Strategies of Three-phase Grid-connected Photovoltaic Systems", *Period. Polytech. Elec. Eng. Comp. Sci.*, 63(3), pp. 213–226, 2019
- [10] M. A. A. M. Zainuri, M. A. M. Radzi, A. CheSoh, N. Mariun, N. AbdRahim, J. Teh and C. Lai "Photovoltaic Integrated Shunt Active Power Filter with Simpler ADALINE Algorithm for Current Harmonic Extraction", *Energies* vol 11, 2018.
- [11] F. J. Lin, K. C. Lu, " Reactive Power Control of Three-Phase Grid-Connected PV System during Grid Faults Using Takagi–Sugeno–Kang Probabilistic Fuzzy Neural Network Control", vol 62, pp 5516-5528, 2015
- [12] S. dahmani, A. semmah, M. kadem, P. wira, "Genetic algorithm optimization of a SAPF based on the fuzzy-DPC concept", *Przegląd Elektrotechniczny*, vol.95, no.7, pp:60-65, 2019.
- [13]. S.Biricik, O.C.Ozerdem, S.Redif and M.O.I.Kmail, "Performance Improvement of Active Power Filter under Distorted and Unbalanced Grid Voltage Conditions", *Journal of Electronics and Electrical Engineering*, Vol. 19, no.1, pp 35-39, 2013.
- [14]. O.C.Ozerdem, S.Biricik "Control of Shunt Active Filter under Nonideal Grid Volage and Un-Balanced Load Conditions," *Electrical, Electronics and Computer Engineering, ELECO 2012*, 29 Nov.-01 Dec. 2012, Turkey.
- [15]. B.Boukezata, A.Chaoui, "Power Quality Improvement by an Active Power Filter in Grid-connected Photovoltaic systems with Optimized Direct Power Control Strategy," *Electric Power Components and Systems*, vol. 44, no. 18, pp.2036-2047.2016.
- [16]. T. Trivedi, R.Jadeja, P. Bhatt. "Improved Direct Power Control of Shunt Active Power Filter with Minimum Reactive Power Variation and Minimum Apparent Power Variation Approaches". *JEET.*; vol 12. No.3: pp.1124-1136, 2017
- [17] B. E. Youcefa, A. Massoum, S. Barkat; S. Bella; P. Wira, "DPC Method For Grid Connected Photovoltaic System Acts as a Shunt Active Power Filter Implemented with Processor in the Loop", *International Conference on Electrical Sciences and Technologies in Maghreb (CISTEM)*, 2018
- [18] B.S.Chen, G. Joos, "Direct Power Control of Active Filters with Averaged switching frequency regulation". *IEEE Trans*, Vol 23, no.6, pp:2729-2737, 2008.
- [19] Y. Komatsu, T. Kawabata. "A Control Method of Active Power Filter in Unsymmetrical Voltage System". *IEEE*. May 1997
- [20] B. Subudhi, R.Pradhan, "A Comparative Study on Maximum Power Point Tracking Techniques for Photovoltaic Power Systems", *IEEE transactions on sustainable energy*, Vol 4 no.1, 2013
- [21] T. Noguchi, H. Tomiki, S. Kondo, and I. Takahashi, "Direct power control of pwm converter without power-source voltage sensors," *IEEE Trans. Ind. Appl.*, vol. 34, no. 3, pp. 473–479, 1998.
- [22]. L. Zhong, M. F. Rahman, W. Y. Hu, and K. W. Lim, "Analysis of direct torque control in permanent magnet synchronous motor drives," *IEEE Transactions on Power Electronics*, vol. 12, no. 3, pp. 528–536, 1997.